Journal of Materials Chemistry C

Accepted Manuscript

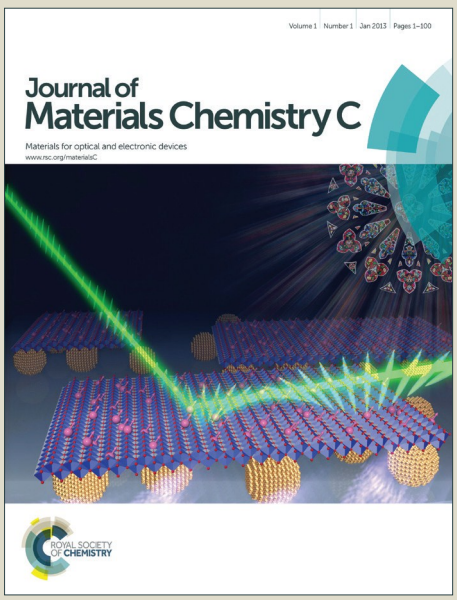

ROYAL SOCIETY OF CHEMISTRY

www.rsc.org/materialsC

Journal Name

RSCPublishing

ARTICLE

Cite this: DOI: 10.1039/x0xx00000x

Received ooth January 2012,
Accepted ooth January 2012

DOI: 10.1039/x0xx00000x

www.rsc.org/

Tailoring melanins for bioelectronics: polycysteinyldopamine as ion conducting redox-responsive polydopamine variant for pro-oxidant thin films.

Nicola Fyodor Della Vecchia,[a] Riccardo Marega,[b] Marianna Ambrico,[d] Mariagrazia Iacomino,[a] Raffaella Micillo,[e] Alessandra Napolitano,[a] Davide Bonifazi,[b,c] Marco d'Ischia[a*]

Polycysteinyldopamine (pCDA), a red hair-inspired polydopamine-like polymer with ionic conductor behavior, can produce smooth and highly adhesive thin films and coatings on quartz, glass and other surfaces, and is shown to markedly accelerate the autoxidation of glutathione at physiological pH via an efficient redox exchange process.

Introduction

The development of multifunctional, adhesive and processable biomaterials that can serve as efficient biointerfaces for transducing signals across the biotic/abiotic gap is currently a major issue in bioelectronics, e.g. for neural interfaces, biosensors, and implantable devices for tissue engineering and regenerative medicine.[1] Although conducting organic polymers are widely employed as biointerfaces, natural or bioinspired materials with intrinsic semiconductor properties appear to offer broader opportunities for future developments and are the focus of intense investigations.[2] In this context, growing interest is attracted by eumelanins, the black subgroup of melanin pigments which arise biosynthetically from tyrosine and which are responsible for the dark colorations of human skin, hair and eyes.[3] The electrical properties of natural and synthetic eumelanins were first described in the 1970s in terms of unusual hydration-dependent amorphous semiconductor-like behavior.[4] Though initially accepted, the amorphous semiconductor model was recently challenged by muon spin relaxation and electron paramagnetic resonance (EPR) data suggesting that eumelanins behave rather as hybrid ionic-electronic conductors.[5] Insights into the redox properties and charge transport mechanisms in synthetic melanins have been reported very recently.[2d,6]

Among the various melanin-based candidate materials for bioelectronic applications, 5,6-dihydroxyindole (DHI) polymers hold considerable interest following development of advanced deposition procedures, such as Ammonia-Induced Solid State Polymerization (AISSP).[2e] Potentially useful, yet little explored opportunities for eumelanin-based organic electronics would derive from polydopamine (pDA) thin films produced by dip-coating of substrates and surfaces into alkaline DA solutions.[7] Because of its multifunctional structural components,[8] robustness, universal adhesion properties and biocompatibility, pDA-based coating technology has opened up the doorway to a borad range of opportunities in biomedicine and nanomedicine, e.g. nanoparticle functionalization, drug delivery and interfacing with cells.[9,10] So far, however, little attention has been directed to develop chemical tailoring strategies aimed at expanding and tuning pDA electrical properties to meet specific requisites for bioelectronic applications. A useful source of inspiration, in this connection, may be provided by the different and uncommon properties of pheomelanins, the reddish-brown subgroup of melanin pigments implicated in the high susceptibility of red haired individuals to sunburn and skin cancer.[11] Red hair pheomelanins arise by the oxidative polymerization of 2*H*-1,4-benzothiazine intermediates derived from 5-*S*-cysteinyldopa, the coupling product of cysteine with dopaquinone (Scheme 1).

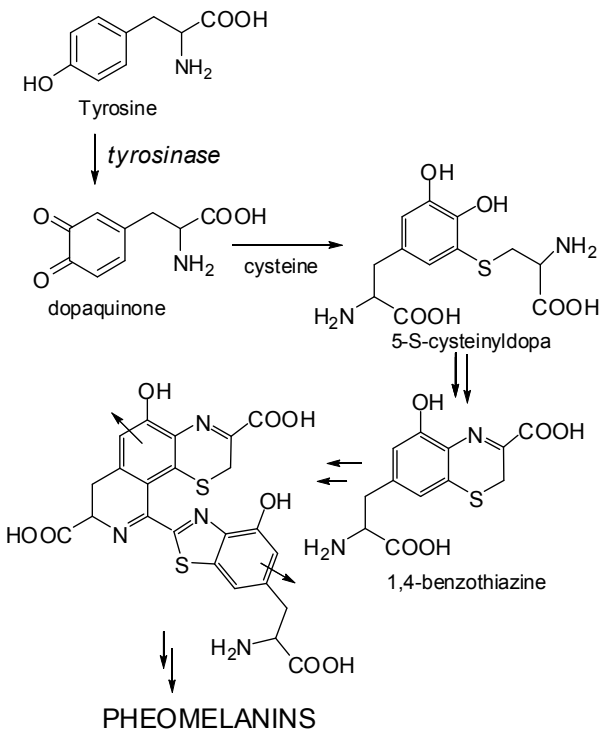

Scheme 1. The pheomelanin biosynthetic pathway, highlighting the formation of benzothiazine intermediates by oxidative cyclization of 5-*S*-cysteinyldopa and their incorporation into pheomelanin structural components.

Both natural and synthetic pheomelanin pigments derived from the oxidation of 5-*S*-cysteinydopa are potent photosensitizers, can promote depletion of key cellular antioxidants, such as glutathione and NADH, and can induce DNA damage by oxygen-dependent, UV-independent mechanisms relying on redox cycling of fundamental 1,4-2*H*-benzothiazine units.[12]
Recently, we reported the copolymerization of dopamine (DA) with 5-*S*-cysteinyldopamine (CDA), the DA-based analog of the red hair pheomelanin precursor 5-*S*-cysteinyldopa, as a convenient chemical tailoring strategy to incorporate pheomelanin-type units in pDA structure (Scheme 2).[13,14]

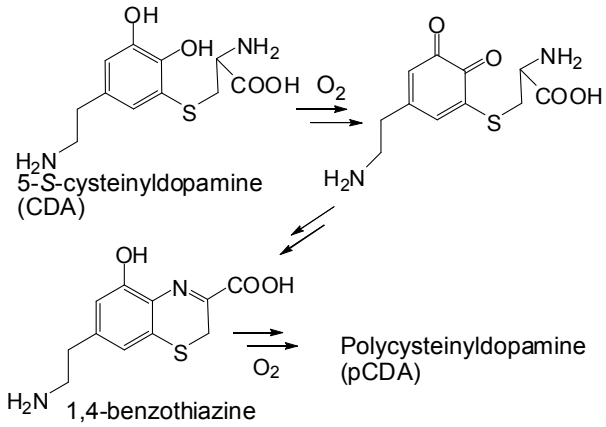

Scheme 2. Structure and oxidation chemistry of CDA leading to pCDA[14b]. The scheme highlights the analogy with the biosynthetic pathway of pheomelanins from cysteinyldopa in Scheme 1, including the formation of benzothiazine intermediates.

CDA was synthesized by a chemical reaction of DA with cysteine under oxidizing conditions. By this approach, it was possible to produce a new pDA variant comprising benzothiazine units similar to those found in photoactive red hair pigments. Experiments carried out using metal-insulator-metal (MIM) and metal-insulator-semiconductor (MIS) devices showed that p(DA/CDA) copolymers exhibit an electrical impedance behaviour resembling that of biological materials and a markedly enhanced photo-capacitive behaviour compared to pDA. Specifically, the introduction of CDA-derived units in pDA potentiated by one order of magnitude the photo-capacitive response of pDA under the application of an AC voltage signal. When inserted in a MIS device on silicon the copolymers proved to serve as a novel 'enhancement layer' for broadband UV-visible detection to implement a solution-processed hybrid photocapacitive/resistive MIS device.[13]
The chemical and electrical properties of pure pCDA, however, were not investigated.
Herein, we report: a) the first use of pure polycysteinyldopamine (pCDA) as a strongly adhesive variant of pDA for dip-coating of glass surfaces via autoxidation of CDA at pH 8.5, i.e. using the reported methodology for pDA;[7] b) the morphological, electrical and chemical characterization of pCDA thin films in comparison with pDA; c) the ability of pCDA thin films to accelerate the autoxidation of two important natural reducing agents, glutathione and NADH, in analogy with the behavior of aqueous suspensions of natural and synthetic pheomelanin polymers.

Results and discussion

Surface functionalization with pCDA and thin film characterization.
CDA, synthesized by a reported method,[15] was allowed to autoxidize at 10 mM concentration in 0.05 M bicarbonate buffer, pH 8.5. Under these conditions, addition of quartz and other materials, e.g. glass, metal objects and plastic cuttings, resulted in deposition of pCDA thin films on their surfaces, as shown in SI (Figure SI-1). Dip-coating of quartz surfaces with pCDA for various periods of time was thus compared with pDA films obtained under the same conditions, up to 24h of polymerization time (Figure 1, top). Solid state UV visible spectra indicate the gradual and polymerization time-dependent generation of a broad band around 400 nm accounting for the lighter yellow-brown coloration of the pCDA films, with respect to pDA. (Figure 1, bottom)

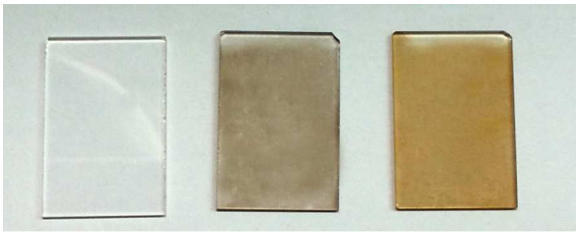

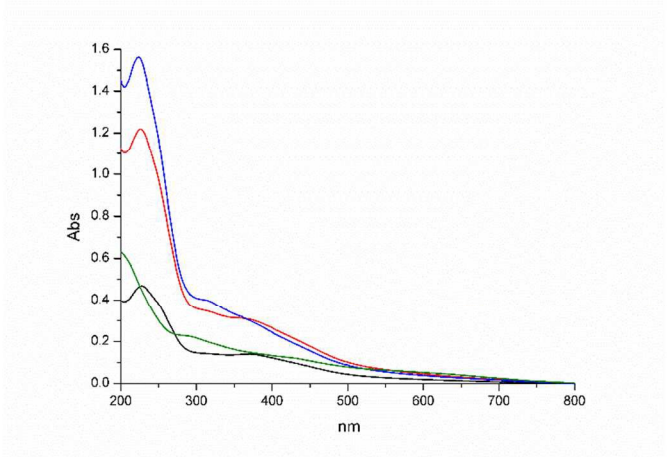

Figure 1. Top: pDA (middle) and pCDA (right) thin films on quartz surfaces produced by oxidation of DA and CDA for 24h against control, no coating (left) Bottom: Solid state UV-vis absorbance spectra of pCDA thin films on quartz obtained at 3 (black line), 6 (red line) and 24 h (blue line) oxidation time and pDA (green line) at 24 h oxidation time.

The morphology of pCDA versus pDA films was investigated by scanning electron microscopy (SEM) and tapping mode atomic force microscopy (AFM) analysis. SEM images revealed similar surface morphology of pCDA and pDA films after oxidation times of 3, 5 and 8 h in the scan range between 100 μm^2 and 3 mm^2 (9,000X and 40X magnifications, respectively, see SI). However, AFM imaging of three areas of 1 μm^2 (randomly selected across the surface) revealed that the pCDA films are much smoother at the nanoscale compared to pDA films. Indeed, fewer agglomerates exceeding the average surface height (around 7 and 10 nm for pCDA and pDA, respectively) were detectable through this imaging method (Figure 2), along with narrower height values frequency distributions (see SI).

Determination of water contact angles (WCA) for thin films obtained after 8 h oxidation time indicated values of 57.8±0.5 for pCDA vs. 42.6±2.8 for pDA, increasing to 73.8±1.1 and 64.0±1.3, respectively, when films were left standing under ambient atmosphere (see also Tables SI-2-7). This may suggest the presence of a certain level of moisture on the as-prepared surfaces, and the convergence of the WCA value for the pDA surface toward the literature reported value of 65 °.[16]

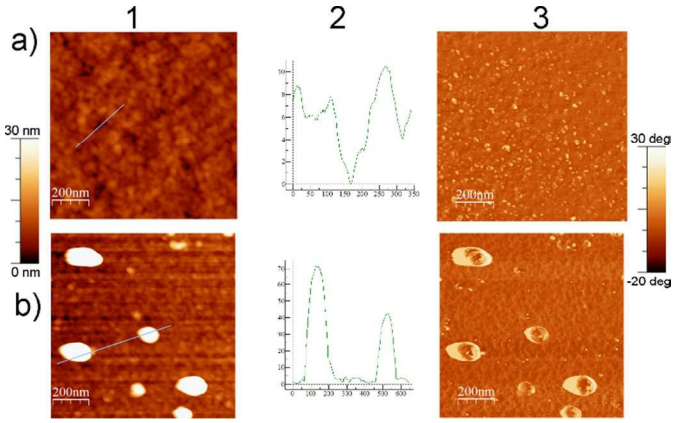

Figure 2 Topography (1) height cross section profile (2) and phase (3) AFM images of pCDA-8h (a) and pDA-8h (b) surfaces. Analysis were performed in air at 298 K on 1 μm^2 areas.

X-ray photoelectron spectroscopy

A detailed chemical characterization of pCDA was reported previously,[13] confirming the formation of benzothiazine and benzothiazole units similar to those found in natural and synthetic pheomelanin pigments. To substantiate this conclusion, and to probe possible structural modifications with time, pCDA thin films were investigated by X-ray photoelectron spectroscopy (XPS). The results confirmed complete retention of sulfur atoms during oxidative polymerization of CDA, with limited variations in compositions (Figure 3). After 8h polymerization a sulfur content of 6.53 ± 0.90 % was determined by XPS. Careful inspection of the S 2p signal (Figure 4) revealed ill-resolved components in the binding energy range of 162-166 eV, while no peak was apparent in the energy region of oxidized sulfur around 168 eV.[17] This result supported the stability of the sulfur-containing structural moieties during polymerization. No sulfur was consistently detected in pDA during polymerization.

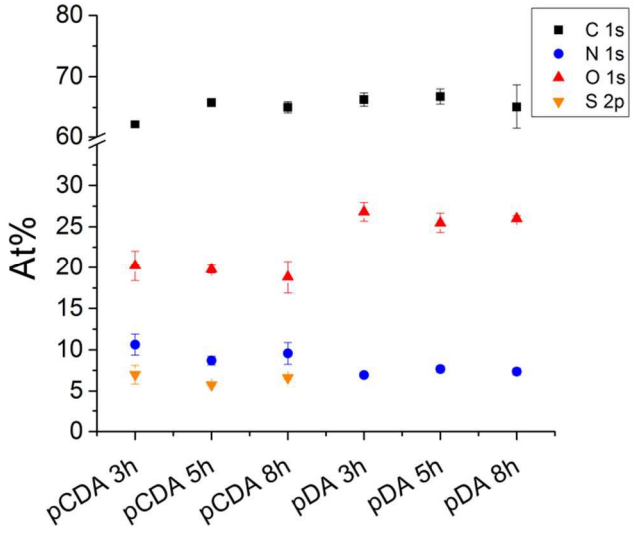

Figure 3. Assessment of the organic moiety composition of pCDA and pDA films on to glass coverslips after 3, 5 and 8 hour of polymerization. At% are reported with black squares for C 1s, red pyramids for N 1s, blue circles for O 1s and orange triangles for S 2p.

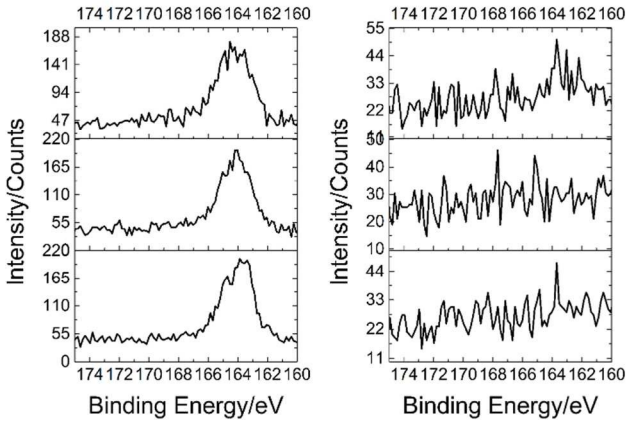

Figure 4. XPS S 2p high resolution spectra of pCDA (left) and pDA (right) films after 8 hours of polymerization onto glass coverslips, collected at three different spots of 250 μm^2.

Overall, chemical and spectral data were consistent with the presence of benzothiazine units within the structure of pCDA as previously reported.[13,14b]

Prooxidant properties of pCDA thin films

Figure 5 shows the effect of pCDA thin films and suspensions on the autoxidation of glutathione (GSH), a primary cellular antioxidant, a substrate for detoxifying enzymes such as glutathione-*S*-tranferase and glyoxalase, and cofactor of glutathione peroxidase, and NADH, a central component of the respiratory chain and a critical index of the metabolic state of the mitochondria. Data showed that pCDA either as thin film or as suspension can markedly accelerate the autoxidation of GSH in phosphate buffer pH 7.4, leading to 65-80 % depletion in less than 3h incubation time, while pDA did not affect the reaction rate significantly. No accelerating effect was observed under an oxygen-depleted atmosphere, indicating an essential role of oxygen in the pCDA-promoted oxidation of GSH. Similar though less marked effects were observed in the case of NADH.

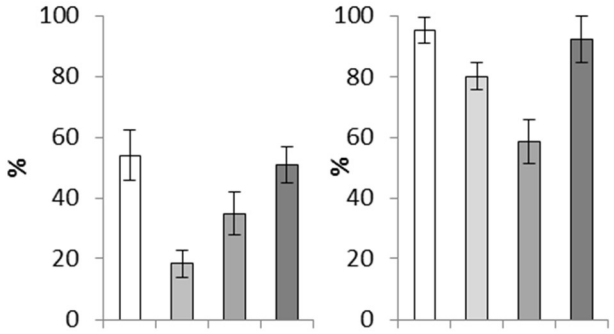

Figure 5. Effect of pCDA on autoxidation of GSH at 150 μM (left panel) and NADH at 300 μM (right panel) at 3 h reaction time in 0.1M phosphate buffer pH 7.4 as determined by HPLC-ED/UV. Shown is residual GSH conc (%). Open bars: control; light grey bars: pCDA thin film; grey bars pCDA as 0.05 mg mL^{-1} suspension; black bars: pDA.

Conductivity properties of pCDA

In a final set of experiments the impedance and AC conductivity properties of pCDA were briefly re-examined in comparison with those of pDA following previously reported experiments.[13] Briefly, the experiments consisted in sandwiching the polymers as dry films obtained by drop casting in between two metallic electrodes (MIM configuration) and by applying an AC modulated voltage.[13] The measured conductance, G(ω) from 1Hz up to 1 MHz was used to calculate the AC conductivity, σ(ω) using the following expression:

$$\sigma(\omega) = G(\omega)\, d/A \qquad (A)$$

where d is the thickness of the sample and A is the cross-sectional area of the electrode. Such a dynamic response is peculiar of disordered materials like ionic conducting glasses,[18] conducting polymers, and also doped crystalline solids [19] and is represented by the universal power law:[20]

$$\sigma(\omega) = \sigma_{dc} + \sigma_{ac}(\omega) \text{ and } \sigma_{ac}(\omega) = A\omega^{s} \qquad (B)$$

where σ_{dc} is the DC conductivity, A is a pre-exponential factor and s is the fractional exponent (relating to the degree of polymer topological imperfection, *i.e.* the higher the defects the lower the s values) whose values are within 0 and 1. The elicited power law fitted the AC conductivities of both pDA and pCDA with a high confidence level. Overall, the AC conductivities showed a plateau in the low frequency region and exhibited dispersion at higher frequencies (Figure 6). The s values were found around 1 in pDA and 0.5 in pCDA (see Table 1) suggesting that both display ionic conductivity mechanisms. In pDA the s value close to 1 indicates that the conducting ion path spans all the sample dimension and drift mechanism is dominant. Conversely, the s value of pCDA evidenced that ion carrier diffusion is inhibited consistently with a tortuous pathway and a more disordered system.

The σ_{dc} that reflects the continuous component (including the electronic one) was almost negligible in pCDA with a slight deviation in the plateau region ascribed to the electrode polarization effect.

The comparison of the Nyquist Plots (NP, data taken at 0.0 V DC bias) gives further insights into the charge transport mechanisms of pDA and pCDA polymers. The NP of pDA, apparently showing one semicircle only, was best fitted with EIS software (see results in SI) by the superposition of two contributions, the first one at high frequency due to ionic resistance in parallel with the layer capacitance; the second one at low frequency due to a very low electron charge transfer resistance (around 50 ohm) and a double layer capacitive contribution. Conversely, NP of pCDA displayed a first semicircle at high frequency, still corresponding to ionic resistance and layer capacitance, and a tail at low frequency, supporting the electron blocking behavior i.e. limited electron charge transfer toward the electrode is present. The high value

of the ionic resistance (R_{HF} hundreds of MΩ, see SI) and high value of Warbourg impedance (see EIS fitting results in S.I., Figure SI 15) suggested an inhibited transport and resistance to diffusion of ionic species. The non-ideal high frequency contribution represented by a constant phase element (CPE) rather than a pure capacitor further underlined that pCDA is a disordered system in agreement with AC conductivity results (s=0.47). The low frequency contribution further shows that charge transfer resistance is higher in pCDA (R_{ct}=53 MΩ, see SI) As a consequence of the electron blocking behavior, under an AC stimulus only charging and discharging of the double layer occurs without faradic reactions. These results agree with the electrode polarization effect (deviation from the plateau) encountered in the low frequency region of the AC conductivity. Interestingly, when considering NP of mixed p(DA/CDA) polymer, a second semicircle is present, suggesting that in the copolymer the pDA components partially weakens the electron blocking behaviour of pCDA and that electron charge transfer mechanism towards the electrode is now allowed (See Figure SI-15).

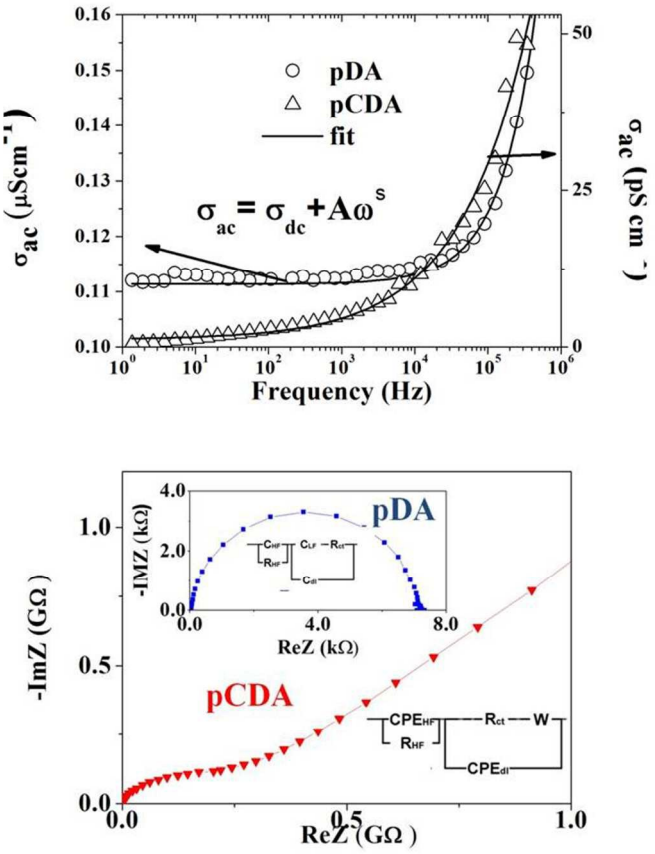

Figure 6. (a) AC conductivities vs frequency for pCDA vs. pDA and fitting curves (continuous lines) by using equation B (b) Nyquist plot experimental data (blue circles: pDA) and red triangles: pCDA)) and fitting transport. Best fitting parameters, corresponding meanings and values are explained and summarized in SI.

Table 1. AC conductivity parameters for pCDA vs, pDA as resulting from fitting of data in Figure 6.

Polymer	σ_{dc}(Scm^{-1})	A	s
pDA	1.12 10^{-7}	1.9 10^{-13}	0.96
pCDA	1.12 10^{-12}	1.3 10^{-13}	0.47

Toward structure-property relationships for polydopamine-based biopolymers

Combining together the results of this and the previous study[13] some important analogies and differences between pCDA and pDA can be highlighted (Table 2).

Table 2. Comparison chart highlighting some basic structure-property relationships for pCDA versus pDA.

	pCDA	**pDA**
Aromatic building blocks	Benzothiazine, benzothiazole	Catecholamine, indole, pyrrole
Main functional groups	o-aminophenol/ o-quinoneimine; NH_2/-NH_3^+; -COOH/-COO^-	QH_2/QH^-/ Q; -NH_2/-NH_3^+; -COOH/-COO^-
Conductivity	Very low, ionic (pS)	Low, electronic-ionic (μS)
Dielectric permittivity (1 Hz-1MHz)	40-0.4	2000-60
Specific Capacitance μFcm^{-2}	0.05	5
Photo-response	LF-HF Modulated photoimpedance effect upon light stimulation	Poor /no response
Increase of GSH autoxidation rate	80%	0%

The key point emerging from Table 2 is that pCDA is more competent to mediate electron exchange by chemical processes, e.g. with thiols, compared to pDA, but is less efficient in mediating electron transport. Such a difference can be ascribed to the different chemistry of the specific redox moieties of pDA and pCDA, namely the catechol-quinone and the *o*-aminophenol-*o*-quinoneimime couples. These related couples operate through free radical intermediates, namely semiquinone and semiquinoneimine (aminophenoxyl radicals), which are believed to be responsible for eumelanin and pheomelanin paramagnetic properties, respectively. Awaiting that new insights into eumelanin conductivity properties become available,[2d] it can be speculated that in pDA catechol/quinone

couples tend to comproportionate in an irreversible hydration-driven manner to give semiquinones that eventually furnish protons and electrons as free charge carriers.[5] This process would evolve until the π-electron system attains an equilibrium condition in which redox exchange, e.g. with thiols, becomes increasingly difficult. Conversely, in pCDA electronic conduction would be limited by the lack of significant comproportionation processes, despite efficient shuttling between different redox states upon interaction with GSH and oxygen [12c,d] (Scheme 3). In pCDA, ionic conductivity would be mainly due to proton transport and may be mediated by protonated amine groups, including the o-aminophenol groups of dihydrobenzothiazine moieties.

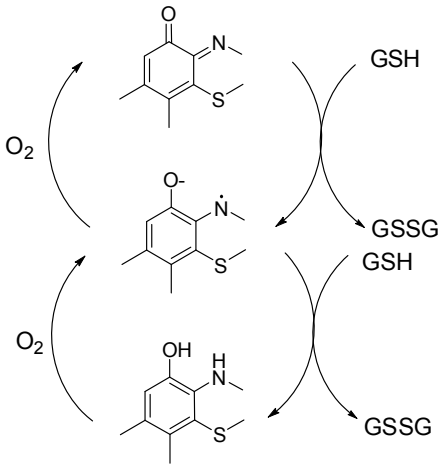

Scheme 3. Schematic illustration of redox cycling mechanisms supposedly involved in pCDA prooxidant properties toward GSH.

Conclusions

The combination of the unique adhesion properties of mussel-inspired eumelanin-type pDA with the redox behavior of benzothiazine systems of red human hair pigments led to the development of pCDA as a novel multifunctional material with remarkable adhesion and pro-oxidant properties. pCDA thin films proved capable of accelerating the kinetics of autoxidation of GSH, a property potentially useful for sensing applications, and is proposed as a novel melanin-based electroactive biomaterial for redox interactions with biomolecules, serving as potential transducer of electrical, redox and luminous signals. Despite the low conductivity, the absence of faradic reactions when sandwiching pCDA in between metallic electrodes and wettability would suggest the implementation of pCDA as a low loss dielectric gate in bio-field effect transistors (bio-FET). More work is necessary to assess biocompatibility and, if required, to overcome limitations in conductivity properties of pCDA in order to implement pCDA-based devices and systems for bioelectronics. However, based on the present and previous data, it can be suggested that while pDA may be suitable to implement signal transducing biointerfaces allowing for significant electron transport, pCDA may be exploited to implement photoresponsive bioelectronic components. The development of biodevices capable of influencing the redox state of cells is also an attractive application of pCDA versus pDA.[10]

Acknowledgements

This work was carried out in the frame of the PRIN 2010-2011 (PROxi project), within the aims of the EuMelaNet special interest group, and of the Belgian National Research Foundation (PACMAN project, n° T.1112.14), the "TINTIN" ARC project from the Belgian French community (Contract No. 09/14-023), the Wallonia Region (THERAPLUS project), the Science Policy Office of the Belgian Federal Government (BELSPO-IAP 7/05 project), the ERC Starting Grant "COLORLANDS". M.A. wishes to thank Paolo Francesco Ambrico and Teresa Ligonzio for their contribution to conductivity experiments, and Mr. Giuseppe Casamassima for technical support. Support from Potenziamento Strutturale PONa3_00369 "Laboratorio per lo Sviluppo Integrato delle Scienze e delle Tecnologie dei Materiali Avanzati e per dispositivi innovativi (SISTEMA)" dell'Università degli Studi di Bari "A. Moro" is gratefully acknowledged. NFDV thanks University of Naples Federico II for financial contribution in support of his stage in Namur University. RM thanks the Fund for Scientific Research (FNRS) of the Wallonia Region (Belgium) for his postdoctoral fellowship.

[a] Department of Chemical Sciences, University of Naples Federico II, Via Cintia 4, I-80126 Naples (Italy) , dischia@unina.it
[b] Namur Research College, University of Namur, Rue de Bruxelles 61, 5000 Namur (Belgium)
[c] Department of Chemical and Pharmaceutical Sciences and INSTM Udr Trieste, University of Trieste, Piazzale Europa 1, 34127 Trieste (Italy)
[d] CNR-Istituto di Metodologie Inorganiche e dei Plasmi, UOS di Bari, Via Orabona 4, 70125 Bari (Italy)
[e] Department of Clinical Medicine and Surgery, University of Naples "Federico II" – Via Pansini 5, I-80131 Naples, Italy .

Electronic Supplementary Information (ESI) available: experimental procedures; SEM, AFM images, elemental distribution maps of pDA/pCDA surfaces, Nyquist plots for p(DA/CDA) –based MIS device. See DOI: 10.1039/b000000x/

Notes and references

1 J Rivnay, R.M. Owens and G.G. Malliaras, *Chem. Mater***.** 2014**, 26**, 679; G Lanzani, *Nature Mater*. 2014, 776.

2 a) C. J. Bettinger, J. P. Bruggeman, A. Misrac, J. T.Borensteind and R. Langer, *Biomaterials*, 2009, **30**, 3050; b) P. Meredith, C. J. Bettinger, M. Irimia-Vladu, A. B. Mostert and P. E. Schwenn, *Rep. Progr. Phys*. 2013, **76**, 034501; c) M. Ambrico, P. F. Ambrico, A. Cardone, T. Ligonzo, S. R. Cicco, R. Di Mundo, V. Augelli and G. M. Farinola, *Adv Mater.* 2011, **23**, 3332; d) J. Wunsche, Y. Deng, P. Kumar, E. Di Mauro, E. Josberger, J. Sayago, A. Pezzella, F. Soavi, F. Cicoira and M. Rolandi, *Chem. Mater.* 2015, **27**, 436; e) A. Pezzella, M., Barra, A. Musto, A. Navarra, M. Alfè, P. Manini, S. Parisi, A. Cassinese, V. Criscuolo, and M. d'Ischia, *Mater. Horizons* 2015, **2**, 212.

3 M. d'Ischia, K. Wakamatsu, A. Napolitano, S. Briganti, J. C. Garcia-Borron, D. Kovacs, P. Meredith, A. Pezzella, M. Picardo, T. Sarna, J. D. Simon and S. Ito, *Pigment Cell Melanoma Res*. 2013, **26**, 616.
4 J. McGinness, *Science*, 1972, **177**, 896.
5 A. B. Mostert, B. J. Powell, F. L Pratt,. G. R. Hanson, T. Sarna, I. R Gentle and P. Meredith, *Proc. Natl. Acad. Sci. USA* 2012, **109**, 8943.
6 G. Tarabella, A. Pezzella, A. Romeo, P. D'Angelo, N. Coppedè, M. Calicchio, M. d'Ischia, R. Mosca and S. Iannotta, *J. Mater. Chem. B* 2013, **1**, 3843-3849.
7 H. Lee, S. M. Dellatore, W. M. Miller and P. B. Messersmith, *Science* 2007, **318**, 426; b) V. Ball, D. Del Frari, M. Michel, M.J. Buehler, V. Toniazzo, M.K. Singh, J. Gracio, D. Ruch, *BioNanoSci.* 2012, **2**, 16.; c) D. R. Dreyer,; Miller, D. J.; Freeman, B.D.; Paul, D.R.; Bielawski, C. W. Perspectives on Poly(dopamine) *Chem. Sci.* **2013**, *4*, 3796-3802
8 a) N.F. Della Vecchia, R. Avolio, M. Alfe, M.E. Errico, A. Napolitano and M. d'Ischia, *Adv. Funct. Mater.* 2013, **23**, 1331; b) C. T. Chen, V. Ball, J. J. de Almeida Gracio, M. K. Singh, V. Toniazzo, D. Ruch, M .J. Buehler, *ACS Nano* 2013, **7**, 1524; c) J. Liebscher, R. Mrówczyński, H.A. Scheidt, C.Filip, N. Hădade, R. Turcu, A. Bende and S. Beck, *Langmuir*, 2013, **29** 10539.
9 a) Y. Liu, K. Ai and L. Lu, *Chem. Rev.* 2014, **114**, 5057; b) K. Kang, S. Lee, R. Kim, I. S. Choi and Y. Nam, *Angew. Chem. Int. Ed.* 2012, **51**, 13101; c) M. d'Ischia, A. Napolitano, V. Ball, C-T., Chen, M.J. Buehler, *Acc. Chem. Res.* 2014, **47**, 3541.
10 a) M. Ramalingama, A. Tiwari, *Adv. Mat. Lett.* 2010, ***1***, 179; b) R. Mout, D. F. Moyano, S. Rana and V. M. Rotello. *Chem. Soc. Rev.*, 2012, **41**, 2539; c) H.-C. Yang, Q-Y. Wu, L.-S. Wana and Z.-K. Xu, *Chem. Commun.*, 2013, **49**, 10522; d) M- J. Salierno, A. J. García and A. del Campo, *Adv. Funct. Mater.* 2013, **23**, 5974.
11 a) A. Napolitano, L. Panzella, L. Leone and M. d'Ischia, *Acc. Chem. Res.*, 2013, **46**, 519; b) G. Greco, L. Panzella, L. Verotta, M. d'Ischia and A. Napolitano, *J. Nat. Prod.* 2011, **74**, 675.
12 a) G. Greco, L. Panzella, G. Gentile, M.E. Errico, C. Carfagna, A. Napolitano and M. d'Ischia, *Chem. Comm*. 2011, **47**, 10308; b) D. Mitra, X. Luo, A. Morgan, J. Wang, M.P. Hoang, J Lo, C.R. Guerrero, J.K. Lennerz, M.C. Mihm, J. A. Wargo, K. C. Robinson, S. P. Devi, J.C. Vanover, J.A. D'Orazio, M. McMahon, M.W. Bosenberg, K.M. Haigis, D.A. Haber, Y, Wang and D.E. Fisher, *Nature*, 2012, **491**, 449; c) L. Panzella, L. Leone, G. Greco, G. Vitiello, G. D'Errico, A. Napolitano and M. d'Ischia *Pigment Cell & Melanoma Res.* 2014, **27**, 244; d) A. Napolitano, L. Panzella, G. Monfrecola and M. d'Ischia, *Pigment Cell & Melanoma Res.*, 2014, **27**, 721.
13 M. Ambrico, N.F. Della Vecchia, P.F. Ambrico, A. Cardone, S.R. Cicco, T. Ligonzo, R. Avolio, A. Napolitano and M. d'Ischia, *Adv. Funct. Mater.* 2014, **24**, 7161.
14 a)K. Wakamatsu, K. Fujikawa, F. A. Zucca, L. Zecca and S. Ito, *J. Neurochem.* 2003, **86**, 1015. b) F. Zhang and G. Dryhurst, *J. Med. Chem.* 1994, **37**, 1084.
15 C. Aureli, T. Cassano, A. Masci, A. Francioso, S. Martire, A. Cocciolo, S. Chichiarelli, A. Romano, S. Gaetani, P. Mancini, M. Fontana, M. d'Erme and L. Mosca, *J. Neurosci. Res*. 2014, **92**, 347.
16 S. H. Ku, J. Ryu, S. K. Hong, H. Lee and C. B. Park, *Biomaterials*, 2010, **31**, 2535.
17 A. Houmam, H. Muhammad and K. M. Koczkur, *Langmuir* 2012, **28**, 16881.
18 S. R. Elliott, *Solid State Ionics* 1988, **27**, 131.
19 a) C. Leon, M. L. Lucıa and J. Santamarıa, *Phys. Rev. B* 1997, **55**, 882; b) C. Leon, M. L. Lucıa, J. Santamarıa, M. A. Parsı, J. Sanz and A. Varez, *Phys. Rev. B* 1996, **54**, 184
20 A. K. Jonscher, *Nature* 1977, **267,** 673; K. A. Mauritz, *Macromolecules* 1989, **22**, 4483.

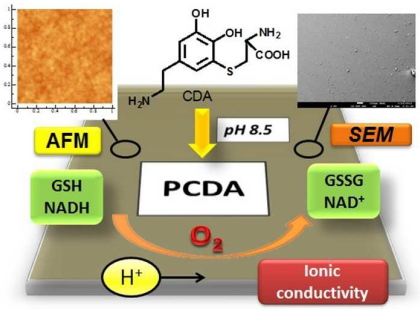

Polycysteinyldopamine (pCDA), a polydopamine-like polymer with ionic conductor behaviour, can be used for dip-coating various surfaces with pro-oxidant thin films